Synthesis and electronic properties of Li doped $LiFePO_4$

J. L. Allen[1], G. V. Zhuang[2], P. N. Ross[2]*, J.-H. Guo[3] and T. R. Jow[1]

[1] Electrochemistry Branch, Sensors and Electron Devices Directorate,
U. S. Army Research Laboratory, Adelphi, MD 20783-1197

[2]Material Science Division and [3]Advanced Light Source
Lawrence Berkeley National Laboratory
Berkeley, California 94720, USA

ABSTRACT

$LiFePO_4$ has several potential advantages in comparison to the transition metal oxide cathode materials used in commercial lithium-ion batteries. However, its low intrinsic electronic conductivity (~ 10^{-9} S/cm) is problematic. We report here a study by soft x-ray absorption/emission spectroscopy of the electronic properties of undoped $LiFePO_4$ and Li-doped $LiFePO_4$ in which Li^+ ions are substituted for Fe^{2+} ions in an attempt to increase the intrinsic electronic conductivity. The conductivities of the $Li_{1+x}Fe_{1-x}PO_4$ samples were, however, essentially unchanged from that of the undoped $LiFePO_4$. Nonetheless, evidence for changing the electronic properties of $LiFePO_4$ by doping with excess Li^+ was observed by the XAS/XES spectroscopy. New pre-edge features the O-*1s* XAS spectrum of $Li_{1.05}Fe_{0.95}PO_4$ is a direct indication that the charge compensation for substitution of Fe^{2+} by Li^+ resides in the unoccupied O-*2p* orbitals. A charge transfer (CT) excitation was also observed in the doped material implying that the unoccupied O-*2p* orbitals created by doping are strongly hybridized with unoccupied Fe-*3d* orbitals of neighboring sites. However, the strong covalent bonding within the $(PO_4)^{3-}$ anions and the large separation of the Fe cations means that the charge created by doping is not delocalized in the manner of electrons or holes in a semiconductor.

*Corresponding author: pnross@lbl.gov

I. INTRODUCTION

Lithium iron phosphate, $LiFePO_4$, was first reported in 1997 by Goodenough as a new cathode material for lithium ion batteries.[1] Since that time, a tremendous research effort has been focused on furthering its development owing to its potential advantages such as a high thermal stability,[2] low reactivity with electrolyte[3-4] and fast recharge capability[5]. It is desirable to replace the standard $LiCoO_2$ cathode material with a cathode based on iron, a less expensive, more abundant and environmentally more acceptable metal than cobalt. The main challenge to the development of $LiFePO_4$ has been its low electronic conductivity ($<10^{-9}$ S/cm). This has been addressed through enhancement of inter-particle conductivity through materials engineering of particle size[6-9] and use conductive carbon coatings. Nonetheless, it would be desirable to increase the bulk electronic conductivity because conductive surface coatings lower the amount of available active material and further lower the already low density (3.6 g/cm^2 versus 5.1 g /cm^2 for $LiCoO_2$)[10].

Recently, enhanced bulk electronic conductivity in $LiFePO_4$ prepared through doping of supervalent cations for lithium was reported[11]. This result has met with controversy as other researchers have suggested that the improvement in conductivity is a result of surface carbon or other impurities that form a conductive network[12, 13]. This controversy stimulated numerous theoretical studies of the electronic structure of $LiFePO_4$ which also had some contradictions. The theoretical situation appears to have been resolved by the work of Zhou *et al*.[14], who also measured the optical band gap using UV-VIS-NIR diffuse reflectance spectroscopy. The result obtained from experiment (3.8 – 4.0 eV) and GGA+U computations (3.7 eV) were in very good agreement. Zhou *et al*. point out that such a large band gap will lead to a very small number of intrinsically generated electrons or holes. They argue further that the carrier concentration in this

material will, therefore, be determined extrinsically, either by impurities, *e.g*. doping, or by Li deficiency, and that most probably any extrinsically generated carriers involved in conduction are not delocalized, but form localized small polarons.

In the present work, we report an experimental study of the electronic structure of undoped and Li-doped $LiFePO_4$ using x-ray absorption (XAS) and x-ray emission (XES) spectroscopies. Our approach was to dope excess lithium into some iron sites to create a new family of the formula $Li_{1+x}Fe_{1-x}PO_4$, with the hypothesis that the substitution of Li^+ onto the Fe^{2+}, M2 site (Fig. 1) would create delocalized hole states thereby increasing the number of charge carriers and improving the conductivity. This approach was also attractive in that no foreign atoms are introduced into the material that may be unstable in the electrochemical environment. XAS probes the unoccupied electronic states, while XES the occupied electronic states. By combining XAS and XES measurement, we could estimate the band gap and determine the orbital character of the doped state. By virtue of photon-excitation and photon-detection, the techniques are applicable to both conducting and insulating samples, a major advantage over electron spectroscopy. We present direct spectroscopic evidence that:

1. the bandgap in $LiFePO_4$ is *ca*. 4 eV consistent with the value reported by Zhou *et al*. from UV reflectance;[14]
2. the charge compensation from extraction/insertion of lithium in Li_xFePO_4 (x = 0,1) is localized entirely on the $Fe^{2+/3+}$ site and there is no hybridization of Fe 3d orbitals with O 2p orbitals;
3. for $Li_{1+x}Fe_{1-x}PO_4$ the excess charge is donated to unoccupied O-*2p* orbitals localized on the M2 site where the Li^+ has substituted for Fe^{2+}.

II. EXPERIMENTAL

We prepared $Li_{1+x}Fe_{1-x}PO_4$ in a range of compositions from x = 0 to 0.05, in the form of sintered pellets, following a method slightly modified from that of Pahdi et al[1]. The $Li_{1+x}Fe_{1-x}PO_4$ samples (x = 0, 0.02, 0.035 and 0.05 were prepared in a two step fashion. Li_2CO_3 (Alfa, 99.0+%), $FeC_2O_4 \cdot 2H_2O$ (Alfa, 99.999%) and $NH_4H_2PO_4$ (Aldrich 99.99+%) were used as starting reagents. Stoichiometric amounts of the powders were mixed in a jar mill for 1 hour utilizing acetone as lubricant. The acetone was evaporated away under a flow of N_2 at room temperature. The resulting intimately mixed powder was then placed in a nickel combustion boat and subsequently heated under N_2 flow for 12 hours at 350^{o}C in a tube furnace. The furnace-cooled reaction mixture was then reground via jar milling for 1 hour in an acetone slurry. The dried powder was now pelletized, placed in an alumina boat and then subjected to a 14 hour heating step at 800^{o}C under a flowing atmosphere of 2.5% H_2 in N_2. The carbon concentration content measured by combustion analysis (Galbraith Laboratories, Knoxville, Tennessee) was found to be 0.26 wt.%, 0.12 wt.% and 0.085 wt.% for the 2%, 3.5% and 5% doped samples, respectively. Thus, the most lithiated material had the least amount of carbon.

Powder diffraction patterns were recorded using Fe $K\alpha_{1,2}$ radiation (λ = 1.9373 Å) on a Philips diffractometer. Data were collected at room temperature by step scanning over the angular range $20^o \leq 2\Theta \leq 70^o$ in increments of 0.02^o in 2Θ. Accurate *d*-spacings of the observed peaks in the X-ray powder diffraction pattern were obtained by use of NIST-traceable silicon as an internal standard. Lattice constants were calculated using a non-linear least squares refinement of the *d*-spacings.

The as synthesized samples were transferred to UHV end-station through loadlock chamber under a helium environment, and measured at ambient temperature without further sample preparation. The base pressure in the experimental chamber was $5x10^{-10}$

torr. The spectroscopic experiments were performed at beamline 7.0.1 at the Advanced Light Source (ALS), Lawrence Berkeley National Laboratory (LBNL)[15]. XAS spectra were measured in fluorescence-yield mode that is more bulk-sensitive than total electron yield mode owing to the larger escape depth of the fluorescent x-ray (about 200 nm and essentially the same as the penetration depth of the incident light). Intensities were normalized to the incident flux using the photocurrent from a gold mesh in the path of photon beam. The energy resolution in XAS was 0.25 eV for the Fe-*2p* absorption and 0.20 eV for the O-*1s* absorption, respectively. The XES spectra were acquired using a high-resolution grazing-incidence spectrometer[16] at energy resolutions of 0.6 eV for Fe *L*-emission and 0.5 eV for O *K*-emission, respectively. A common energy scale for XAS and XES spectra was established by determining the peak positions of elastically scattered X-rays in resonant X-ray emission spectra.

III. RESULTS

A. Structural and Electrical Characterization

The detailed crystal structure is shown in Fig.1. Within the crystal structure, P atoms are tetrahedrally-coordinated by oxygen forming PO_4, and Fe and Li atoms are octahedrally-coordinated by oxygen atoms forming FeO_6 and LiO_6. FeO_6 octahedra are interconnected via corner sharing along the bc-plane and have two common edges with LiO_6 octahedra and one PO_4 tetrahedron, where Fe atoms occupy M2 sites and Li atoms occupy M1 sites. All the peaks in the x-ray powder diffraction patterns (XRD) (Fig. 2), can be indexed to the phospho-olivine structure. $LiFePO_4$ has an orthorhombic crystal structure with Pnma space group and lattice constants of a=10.329 Å; b=6.007 Å; c= 4.6908 Å.

The DC resistance of sintered parallelepipeds was measured by the four-probe method. The absolute value of the conductivity of powdered materials is inherently a

measure of the resistance of the composite material which may contain surface phases or phases within the grain boundary which have high conductivity but are amorphous or of too low concentration to be detected by XRD. These impurities could form a conductive network. As was pointed out by Nazar *et al.*[13], possible impurities include carbon present in the starting materials and iron phosphides formed by reduction during the synthesis. To minimize the contribution of surface phases, the $Li_{1+x}Fe_{1-x}PO_4$ pellets from the final step of synthesis were re-ground to fine powders then formed into sintered parallelpipeds for the conductivity measurements. The conductivity of the $Li_{1+x}Fe_{1-x}PO_4$ samples was essentially unchanged from that of the undoped $LiFePO_4$, which is lower than we could accurately measure with our apparatus, i.e. $< 10^{-9}$ S/cm.

B. X-ray Absorption (XAS) and X-ray Emission (XES)

The electronic structures of $FePO_4$, $LiFePO_4$ and $Li_{1.05}Fe_{0.95}PO_4$ were studied using x-ray absorption spectroscopy and x-ray emission spectroscopy. XAS and XES provide information with elemental selectivity due to the involvement of inner shell electrons and with chemical sensitivity due to the involvement of valence electrons. Thus, the local electronic structure of selected elements in a complex material can be examined.

Fe $L_{2,3}$ edge XAS and Fe XES

Fe-*2p* XAS spectra of $LiFePO_4$ and $Li_{1.05}Fe_{0.95}PO_4$ are shown in Fig. 3. The absorption features in the region of 705 eV- 718 eV, with a main peak at 708 eV, originate from the transitions of Fe $2p_{3/2} \rightarrow 3d$ (L_3 edge), and those in the region of 718 eV– 731 eV, with main peak at 721 eV, are from the transitions of Fe $2p_{1/2} \rightarrow 3d$ (L_2 edge). The XAS spectrum of $FePO_4$ shows a sharper main absorption peak at 710 eV, which is shifted by about 2 eV to higher photon energy with respect to that of $LiFePO_4$.

The Fe-*2p* absorption has been a subject of considerable theoretical study and has been shown to be highly sensitive to the local symmetry of the Fe site and its formal

valency,[17,18] based upon crystal field treatment in combination of atomic multiple theory. The Fe-*2p* absorption spectra of both $LiFePO_4$ and $Li_{1.05}Fe_{0.95}PO_4$ are in good agreement with the theoretical prediction for Fe^{2+} in octahedral site (O_h) with a cubic crystal-field parameter (10Dq) of 1-1.5, while that of $FePO_4$ with the theoretical prediction for Fe^{3+} in octahedral site (O_h) with a cubic crystal -field parameter (10Dq) of 1-1.5. The difference between $Li_{1+x}Fe_{1-x}PO_4$ (x = 0 and x = 0.05) lies in the intensity reduction at ~711 eV in Fe L_3-edge for the x = 0.05 sample. If there has been a change in valency from Fe^{2+} to Fe^{3+} upon Li doping, an intensity enhancement at 710 eV would be observed, at which energy XAS is most sensitive to Fe^{3+}. Instead, an intensity reduction was observed in this energy region in comparing $LiFePO_4$ to $Li_{1.05}Fe_{0.95}PO_4$. Thus, the evidence from X-ray absorption measurements indicates there is no Fe^{+3} valence in $Li_{1.05}Fe_{0.95}PO_4$ upon excess Li^+ doping. A possible interpretation of the XAS spectra is that there is different crystal-field strength in $LiFePO_4$ and $Li_{1.05}Fe_{0.95}PO_4$ originating from a lattice distortion as a result of Li^+ substitution into the Fe^{2+} site[17,18].

Fig.4 shows XES spectra of $Li_{1.05}Fe_{0.95}PO_4$ (solid line) excited at energies indicated by the arrows in the XAS spectrum (upper panel, Fig. 4). Spectra of $LiFePO_4$ (dashed line) obtained at the same excitation energies were also shown for comparison. The resonantly excited X-ray emission spectra are plotted on an energy-loss scale (with respect to photon excitation energy), where peaks at constant energy loss arise from scattering processes and peaks that disperse with energy arise from normal emission from the occupied Fe 3d states. There is strong variation in the intensities of these processes depending on the excitation energies. By resonant excitation below Fe L_2 edge (curves A-F in Fig. 4), the complication of normal emission was largely eliminated. Two distinctive loss features centered at -3 eV and -5.5 eV originate from *d-d* excitations of Raman scattering, based on crystal-field multiplet calculations for $LiFePO_4$[19]. The broad loss

feature centered at ~ -9 eV, at excitation energy A, was assigned to charge transfer (CT) excitation of final state character in $LiFePO_4$[20]. The normal emission contribution from the Fe 3d states, as indicated by the dispersive feature in the energy loss scale marked by short solid lines, are only observed at excitation energies above the ionization threshold of Fe the L_3-edge, *i.e.*, at excitation energies between G-J. The normal emission features are not well-resolved in these spectra and do not accurately reflect the Fe-*3d* partial DOS of $LiFePO_4$[14]. There is no significant spectral difference between undoped and 5% Li doped $LiFePO_4$ samples at resonant excitation energies below the Fe L_3-edge, points A – F. Most striking is the fact that both doped and undoped samples yield virtually identical X-ray emission spectral profiles at selected excitation energies, where the contribution of Fe^{+3} would be revealed if present. Thus the data does not present any evidence of formal Fe valency change upon excess Li doping, consistent with XAS spectral evidence presented in Fig. 3. However, discernable emission intensity difference appears as excitation energy is tuned to G. A new feature at ca. -7 eV in energy loss scale, unique to doped $Li_{1.05}Fe_{0.95}$ PO_4, was observed. This loss feature is also registered strongly in the oxygen XES, and can be assigned to charge transfer (CT) excitation which will be discussed in more detail later.

***O K-edge XAS* and XES**

The O-*1s* absorption and *K*-emission spectra of $LiFePO_4$ and $Li_{1.05}Fe_{0.95}PO_4$ are displayed in Fig. 5a. It is well known[21] that features in the so-called pre-edge region of 530 –535 eV in the O-*1s* absorption spectra of transition metal oxides are the result of hybridization of O-*2p* and metal *3d* states, and that the X-ray absorption intensity in this region is a measure of the hybridization strength of these materials. Indeed, O-*1s* absorption spectra of $Fe^{2+/3+}$ oxides, such as Fe_2O_3 and Fe_3O_4, have strong absorption in the pre-edge region[21, 22]. In the undoped $LiFePO_4$, there is no significant absorption in

this region of the XAS spectrum, indicating less hybridization between Fe-*3d* and O-*2p* in this material. In the O-*1s* absorption spectrum of the doped $Li_{1.05}Fe_{0.95}PO_4$, there are new pre-edge absorption features (denoted A and B) which are not observed in the undoped $LiFePO_4$ nor in Li_2O[23], which we assign to new states in the unoccupied O-*2p* density of states created by doping with excess Li^+. Thus, these states are empty (acceptor or hole) states in the doped material lying about 1 eV above the valence band edge (at 530 eV in the energy scale of Fig. 5a). If these states form a bulk band, which may not be determined just from the XAS spectrum only, these doping states would be expected to impart p-type electronic conductivity.

We further probe the nature of the doping states residing in the unoccupied O-*2p* band by resonant X-ray emission spectroscopy by measuring X-ray emission spectra of $LiFePO_4$ and $Li_{1.05}Fe_{0.95}PO_4$ at the excitation energies corresponding to A, B and C in the XAS spectrum Fig. 5a. These resonant X-ray emission spectra of $LiFePO_4$ and $Li_{1.05}Fe_{0.95}PO_4$ are presented in Fig. 5b-5d, in which all the spectra were normalized to the incident photon flux. Excitation into the unoccupied state corresponding to C produces non-resonant (normal) emission in both the doped and undoped materials, with identical spectral profiles (Fig. 5d) that reflects essentially identical structure in the occupied O-*2p* states. The normal emission profiles consist of a strong main band at 526 eV with a strong shoulder at its low energy side, and a weaker lobe at 522 eV with a tail. The former originates from O-*2p* and Fe-*3d* derived states and the latter arises from O *2p* – Fe *3d* hybridization states, as well as O-*2p* – P-3*p*, O-*2p* – Li-2*s* and O-*2p* – Li-2*p* hybridization states.[19] In contrast to $LiFePO_4$, X-ray emissions from $Li_{1.05}Fe_{0.95}PO_4$ at excitation energies A and B (Fig. 5b and c) have very different behavior in that they exhibit increased intensity, which comes from an increased cross-section, characteristic of resonant excitation. Specifically, resonant emission spectra of $Li_{1.05}Fe_{0.95}PO_4$ consist of

several characteristic features. The X-ray emission bands that are independent of photon excitation energy (main bands at 522 eV and 526 eV) represent O-*1s* excitation into continuous band-like final states, while the small features marked by downwards arrows are the elastic scattering peaks at photon excitation energy of 531 eV (A) and 532 eV (B). The features shifting with photon energy (dispersive), as indicated by upward arrows, warrant further detailed discussion.

When there is resonant excitation to the unoccupied state corresponding to A in XAS spectrum of $Li_{1.05}Fe_{0.95}PO_4$, a sharp emission peak appears at 524 eV (Fig. 5b), which is a very minor feature in the normal emission in Fig. 5d. This sharp peak in Fig. 5b is attributed to a charge transfer (CT) excitation[24], where the CT process is illustrated schematically in Fig. 6. When a valence electron fills the O-*1s* core-hole created by the resonant excitation A, there is an accompanying electron transfer of an O-*2p* electron to an unoccupied Fe-*3d* state. This electron transfer needs additional energy to overcome the potential barrier, which would behave as an energy loss of about 7 eV, with respect to the elastic peak at 531 eV, in the resonant inelastic scattering process, as illustrated in Figure 6. When the photon energy is increased by 1 eV to B, the energy-loss feature follows the shift, but the intensity of the CT feature (remaining at an energy loss of 7 eV) is much reduced. The similar CT process in O K-edge emission has been reported for other complex oxides, most notably $CuGeO_3$[25]. The CT excitation in the doped material implies that the unoccupied O-*2p* orbitals created by doping are strongly hybridized with unoccupied Fe-*3d* orbitals of neighboring sites.

IV. DISCUSSION

We discuss first the problem of surface phases and their effect on the XAS/XES spectra. In a previous study[19] of the electronic properties of $LiFePO_4$ also using XAS/XES, a different sample of $LiFePO_4$ was used versus that used here. The sample in

the earlier study was obtained from Hydro-Quebec, and we did not realize at the time that this material has by design a "conductive coating" to promote inter-particle electronic conduction[6]. The $LiFePO_4$ material studied in this work was synthesized at Army Research Laboratory (ARL) using a procedure designed to produce a pure sample free from impurities or surface phases. The O-*1s* XAS spectrum from the Hydro-Quebec sample reported previously had pre-edge features which subsequent study clearly showed were from the oxygen atoms in the "conductive coating" and not characteristic of $LiFePO_4$.

The lattice constant change observed at compositions where $x > 0$ in $Li_{1+x}Fe_{1-x}PO_4$ provides the first indication of doping though it can not be taken as sole confirmation of doping owing to the fact that it is at the limit of instrumental resolution. If one considers, the $LiMPO_4$ structure which is adopted by M = Ni, Mg, Co, Fe and Mn in order of increasing ionic radius, the most sensitive lattice constant to the ionic radius of M is the *b* lattice constant. Even so, the *b* lattice of $LiNiPO_4$ (Ni^{2+} radius of 0.83 Å) is only 2.95% smaller than $LiFePO_4$ (Fe^{2+} radius = 0.92 Å). Thus, the lattice constant change resulting from substitution of Li^+ (radius = 0.90 Å) for Fe^{2+} at 5% doping will be practically immeasurable. One can calculate a difference of 0.03% based on an imaginary cation of radius 0.919 Å, the ionic radius calculated via a weighted average based on the 95% Fe, 5% Li composition. We did observe a very slight contraction in the unit cell volume that is in accordance with the slightly smaller size of the Li^+ ion replacing of Fe^{2+} ion in the M2 site[25], but the change is not outside the measurement error.

The primary evidence for changing the electronic properties of $LiFePO_4$ by doping with excess Li^+ is primarily from the XAS/XES spectroscopy. The new pre-edge features denoted A and B in the O-*1s* XAS spectrum of $Li_{1.05}Fe_{0.95}PO_4$ is a direct indication that the charge compensation for substitution of Fe^{2+} by Li^+ resides in the

unoccupied O-*2p* orbitals. In a classic semiconductor, unoccupied states appearing in the band gap upon doping are regarded as acceptor or hole states, and would impart p-type electronic conductivity. However, the CT excitation we observed in the doped material implies that the unoccupied O-*2p* orbitals created by doping are strongly hybridized with unoccupied Fe-*3d* orbitals of neighboring sites. In cuprates like $CuGeO_3$, the hybridization of unoccupied Cu-*3d* and O-*2p* form what is called the upper Hubbard band (UHB), although these materials are insulators (at room temperature) because the band is about 3 eV above the Fermi level[25]. However, the relatively narrow line-width of the CT excitation in $Li_{1.05}Fe_{0.95}PO_4$ implies that the doped state is not delocalized, i.e. localized on the oxygen atoms surrounding the Li^+ substituted M2 site. However, the question of the localization versus delocalization of the charge imbalance created by doping requires further detailed consideration.

Goodenough and co-workers[1] have argued that in Fe-based compounds with $(XO_4)^{n-}$ polyanions, the polarization of the electrons of the O^{2-} ions into strong covalent bonding within the polyanion reduces the covalent bonding to the Fe ion and influences the redox potential of the Fe^{2+}/Fe^{3+} couple. Because the P – O covalent bonding is relatively strong in $(PO_4)^{3-}$, it is inferred that the Fe – O interaction is relatively weak, and consequently the $LiFePO_4$ redox potential is strongly shifted relative to other Fe^{2+}/Fe^{3+} compounds. The observation in this work of increased Fe – O hybridization in the Li-doped material is another manifestation of a related inductive effect. Substitution of Li^+ for Fe^{2+} results in a local charge imbalance around the $(PO_4)^{3-}$, *i.e.* "missing" positive charge, that appears to be compensated by increased covalent bonding (hybridization) between Fe^{2+} and O^{2-} ions. The CT excitation in the Li-doped material implies that the unoccupied Fe d-orbitals are pulled down closer to the Fermi level by the Li doping, inducing Fe^{2+} cations to have partially Fe^{3+} electronic character, *i.e.* $Fe^{2.5+}$. The distortion

of the electron distribution on the $(PO_4)^{3-}$ anions due to the cationic charge imbalance also has a compensating effect on the orbitals of the O^{2-} ions surrounding the Li^+ in the M2 site. These ions have "excess" electron density relative to the undoped state resulting in partial filling of the unoccupied O-*2p* orbitals and appearance of new states in the band gap of the undoped material. None of these considerations however give any indication that the charge imbalance induced by Li^+ substitution into an M2 site is delocalized beyond the adjacent $(PO_4)^{3-}$ anions.

Based on the relatively large band gap of 3.9 eV in $LiFePO_4$, Zhou *et al*. argued that the carrier concentration in this material would always be determined extrinsically versus intrinsically, either by impurities, or more likely, by Li deficiency. Based on their electronic structure calculations, they conclude that charge created by Li deficiency is not delocalized, but rather forms localized small polarons, and that the electron conductivity is determined by the polaron mobility, *i.e*. the hopping rate of the polarons. Although Zhou *et al*. do not state this, it is implicit in their discussion of the electronic structure of $LiFePO_4$ that the strong covalent bonding within the $(PO_4)^{3-}$ anions and the large separation of the Fe cations means that any charge imbalance created extrinsically, regardless of the means, is not delocalized in the manner of electrons or holes in a semiconductor. Rather, any charge created extrinsically in this material will form a small polaron which have much lower (orders of magnitude) mobility than a charge carrier in a semiconductor[27].

V. CONCLUSIONS

The conductivities of the $Li_{1+x}Fe_{1-x}PO_4$ samples were essentially unchanged from that of the undoped $LiFePO_4$, which is lower than we could accurately measure with our apparatus, *i.e*. $< 10^{-9}$ S/cm. Nonetheless, evidence for changing the electronic properties of $LiFePO_4$ by doping with excess Li^+ was observed by the XAS/XES spectroscopy. New

pre-edge features in the O-*1s* XAS spectrum of $Li_{1.05}Fe_{0.95}PO_4$ are a direct indication that the charge compensation for substitution of Fe^{2+} by Li^{+} resides in the unoccupied O-*2p* orbitals. A charge transfer (CT) excitation was also observed in the doped material implying that the unoccupied O-*2p* orbitals created by doping are strongly hybridized with unoccupied Fe-*3d* orbitals of neighboring sites. However, the strong covalent bonding within the $(PO_4)^{3-}$ anions and the large separation of the Fe cations means that the charge created by doping is not delocalized in the manner of electrons or holes in a semiconductor. It appears based on fundamental considerations that any charge created extrinsically in this material will form a small polaron which have much lower (orders of magnitude) mobility than a charge carrier in a semiconductor.

Acknowledgements: We thank K. Xu, S. Zhang, M. Ding and J. Wolfenstine and Marca Doeff for useful discussions and we thank C. L. Dong and C. L. Chang of Tamkang University for assistance with the x-ray spectroscopy experiments. Financial support from Chemical Sciences Division (GVZ and PNR) and the Materials Sciences Division (JHG) of the Office of Basic Energy Sciences, U.S. Department of Energy, under contract No. DE-AC02-05CH11231 is gratefully acknowledged.

REFERENCES

1. A.K. Pahdi, K.S. Nanjundaswamy, and J. B. Goodenough, J. Electrochem. Soc., **144**, 1188 (1997).
2. A. S. Andersson, J.O. Thomas, B. Kalska, and L. Häggström, Electrochem. Solid State Lett., **3**(2), 66 (2000).
3. D. D. MacNeil, Z. Lu, Z. Chen, and J.R. Dahn, J. Power Sources, **108**(1-2), 8 (2002).
4. M. Takahashi, S. Tobishima, K. Takei, and Y. Sakurai, Solid State Ionics **148** (3-4), 283 (2002).
5. A. Yamada, M. Yonemura, Y. Takei, N. Sonoyama, R. Kanno**,** Electrochem. Solid State Lett., **8**(1), A55 (2005).
6. N. Ravet, Y. Chouinard, J. F. Magnan, S. Besner, M. Gauthier and M. Armand, J. Power Sources, **97-98,** 503 (2001).
7. H. Huang, S.-C. Yin, and L.F. Nazar, Electrochem. Solid State Lett., **4**(10), A170 (2001).
8. P. P. Prosini, D. Zane, and M. Pasquali, Electrochim. Acta, **46**, 3517 (2001).
9. A. Yamada, S.C. Chung, and K. Hinokuma, J. Electrochem. Soc., **148**(3), A224 (2001).
10. Z. H. Chen, J.R. Dahn, J. Electrochem. Soc., **149**(9), A1184 (2002).
11. S.-Y Chung, J.T. Bloking, and Y.-M. Chiang, Nat. Mater. **1**, 123-128 (2002).
12. N. Ravet, A. Abouimrane, and M. Armand, Nat. Mater. **2**, 702 (2003).
13. P.S. Herle. B. Ellis, N. Coombs, and L.F. Nazar, Nat. Mater. **3**, 147-152 (2004).
14. F. Zhou, K. Kang, T. Maxisch, G. Ceder and D. Morgan, *Solid State Comm.* **132**, 181 (2004).

15. T. Warwick, P. Heimann, D. Mossessian, R. Nyholm, W. McKinney, H. Padmore, Rev. Sci. Instrum., **66,** 2037 (1995).

16. J. Nordgren, G. Bray, S. Cramm, R. Nyholm, J.-E. Rubensson, and N. Wassdahl Rev. Sci. Instrum., **60,** 1690 (1989).

17. F. M. F de Groot, J. C. Fuggle, B. T. Thole, and G. A. Sawatzky, Phys. Rev. B, **42,** 5459 (1990).

18. G. van der Laan and I. W. Kirkman, J. Phys.: Condens. Matter, **4**, 4189 (1992).

19. A. Augustsson, G. V. Zhuang, S. M. Butorin, J. M. Osorio-Guillén, C. L. Dong, R. Ahuja, C. L. Chang, P. N. Ross, J. Nordgren and J.-H. Guo, J. Chem. Phys., **123,** 184717 (2005).

20. S. M. Butorin, J. Electro Spectroc. and Relat. Phenom. **110-111,** 213 (2000).

21. F.M.F. de Groot, M. Grioni, J.C. Fuggle, J. Ghijsen, G.A. Sawatzky, and H. Petersen, Phys. Rev. B, **40,** 5715 (1989).

22. Z. Y. Wu, S. Gota, F. Jollet, M. Pollak, and M. Gautier-Soyer, Phys. Rev. B, **55,** 2570 (200).

23. P. Kuiper, G. Kruizinga, J. Ghijsen, G.A. Sawazky, and H. Verweij, Phys. Rev. Lett., **62,** 221 (1989).

24. L.-C. Duda, T. Schmitt, A. Augustsson and J. Nordgren, J. Alloys and Compounds, **362**, 116 (2004).

25. L.-C Duda, J. Downes, C. McGuinness, T. Schmitt, A. Augustsson, K.E. Smith, G. Dhalenne and A. Revcolevschi, Phys. Rev. B, **61,** 4186 (2000).

26. R. D. Shannon, Acta Crystallogr. **A32**, 751 (1976).

27. A. L. Shluger and A. M. Stoneham, J. Phys.: Condens. Matter **5**, 3049-3086 (1993).

Figure Captions

Figure 1. Ordered $LiFePO_4$ olivine structure: *Pnma* spacegroup with Li in M1 octahedral site, Fe in M2 octahedral site, P in tetrahedral site represented by tetrahedron.

Figure 2. X-ray diffraction pattern of $Li_{1+x}Fe_{1-x}PO_4$ samples where x = 0 (0%), 0.02 (2%), 0.035 (3.5%) and 0.05 (5%). The peaks are labeled with Miller indices corresponding to the phospho-olivine phase, space group *Pnma*.

Figure 3. Fe-2p X-ray absorption spectra of $FePO_4$, $LiFePO_4$ and $Li_{1.05}Fe_{0.95}PO_4$.

Figure 4. XAS and RXES of $Li_{1+x}Fe_{1-x}PO_4$ (x=0 and 0.05) at Fe L-edge. The RXES are plotted in energy loss scale. Energy loss feature marked as (*) at -7 eV is assigned to the charge transfer (CT) excitation in Figure 6.

Figure 5. O-1s absorption and K-emission spectra of $LiFePO_4$ and $Li_{1.05}Fe_{0.95}PO_4$ (a); Resonantly excited O K-emission spectra at excitation energies of positions A (b) and B (c); and normal O K-emission spectra (d).

Figure 6. Resonant inelastic X-ray scattering and charge transfer (CT) process of Li doped $LiFePO_4$.

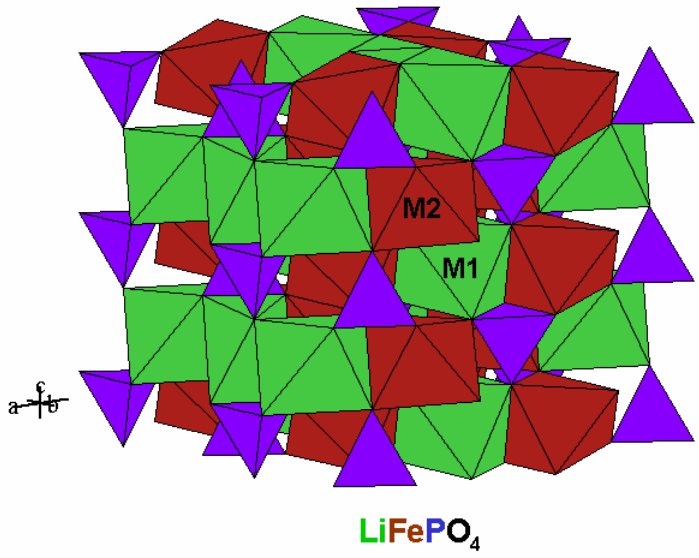

Figure 1

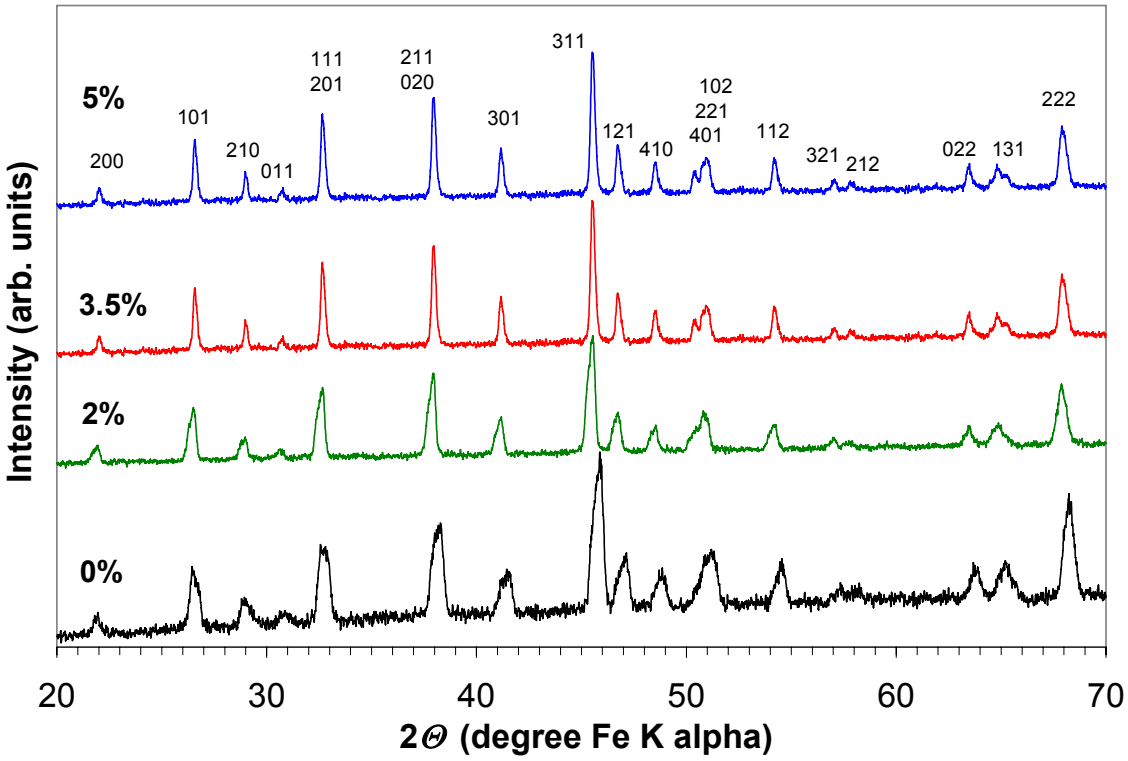
5%
3.5%
2%
0%
200
101
210
011
111
201
211
020
301
311
121
410
102
221
401
112
321
212
022
131
222
Intensity (arb. units)
20
30
40
50
60
70
2Θ (degree Fe K alpha)

Figure 2

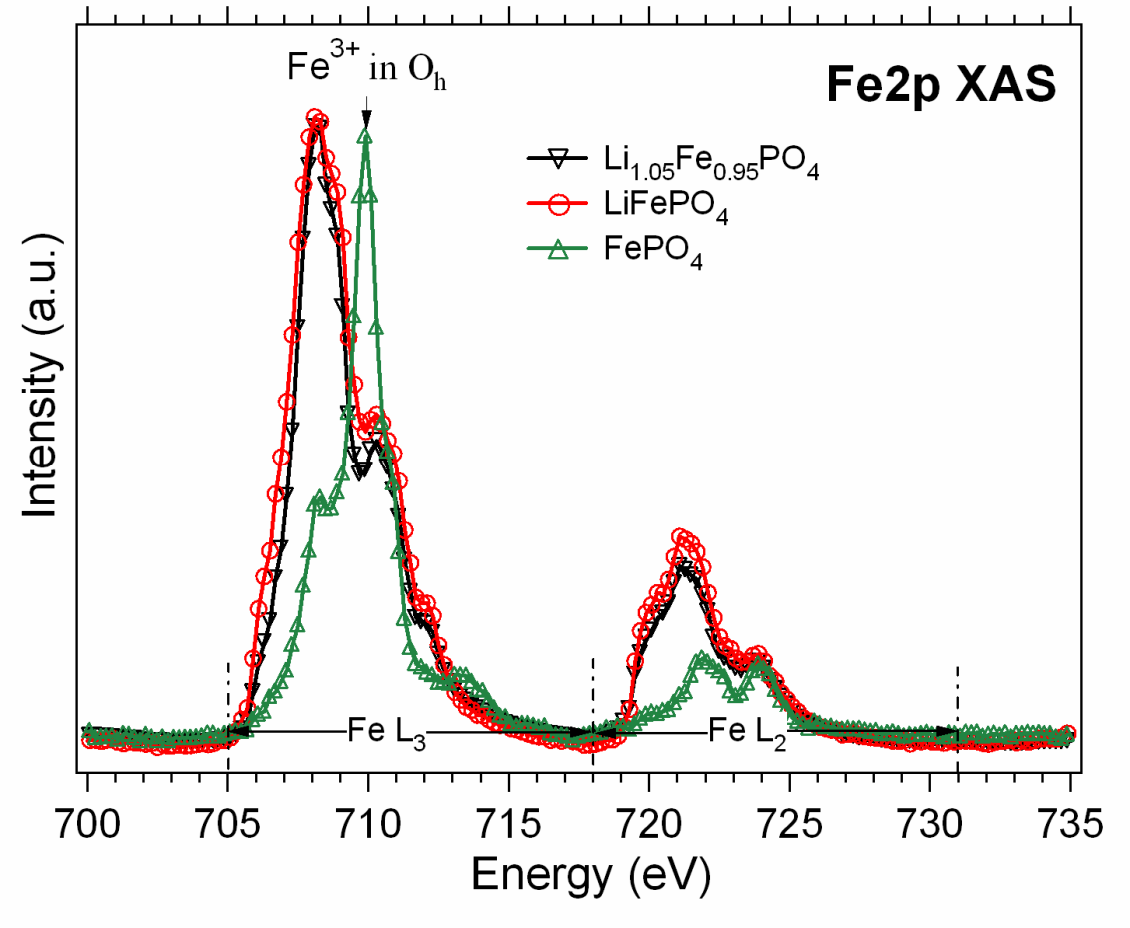
Fe2p XAS
Fe3+ in Oh
Li1.05Fe0.95PO4
LiFePO4
FePO4
Fe L3
Fe L2
Intensity (a.u.)
Energy (eV)
700
705
710
715
720
725
730
735

Figure 3

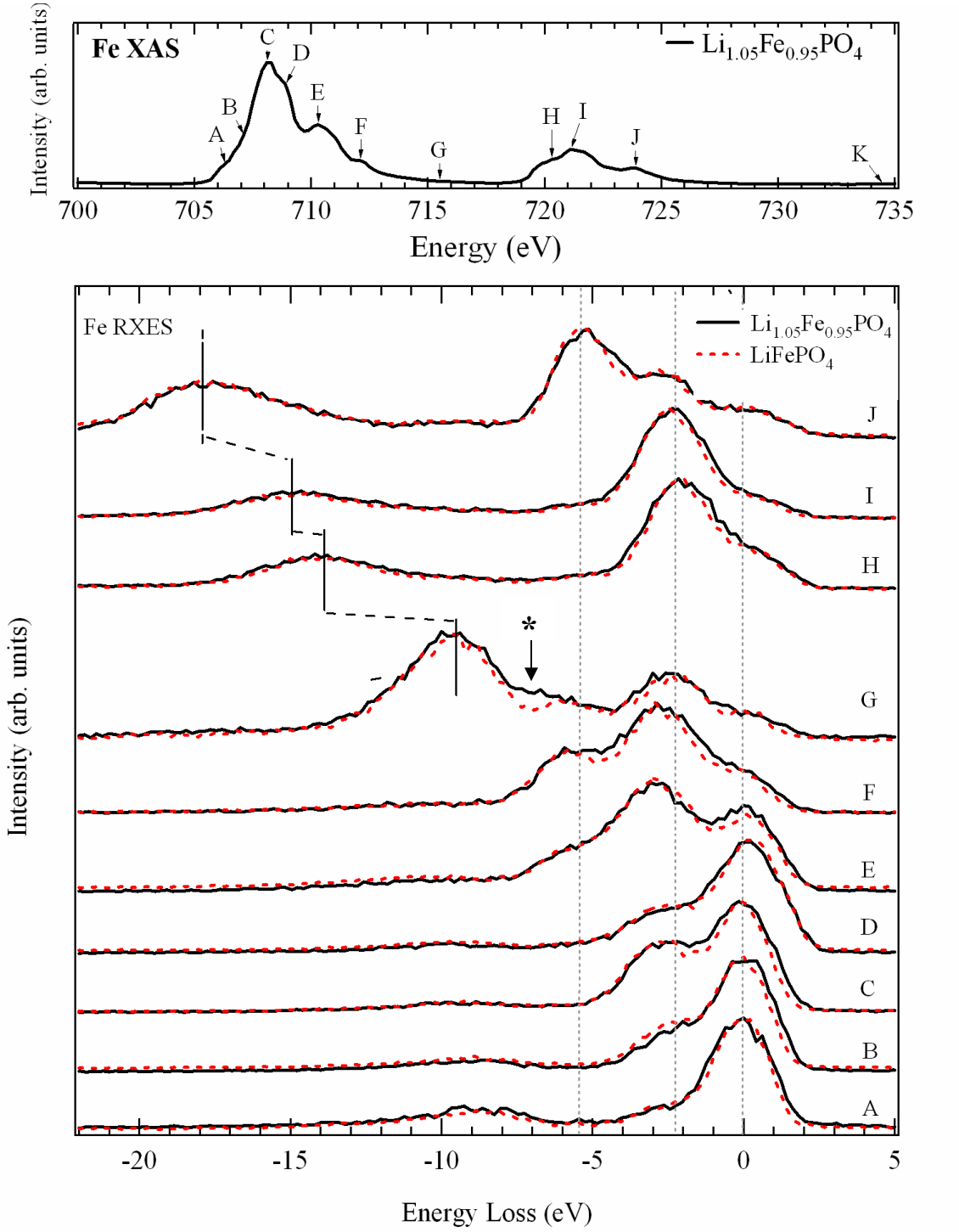
Fe XAS
Li1.05Fe0.95PO4
A
B
C
D
E
F
G
H
I
J
K
Intensity (arb. units)
700
705
710
715
720
725
730
735
Energy (eV)
Fe RXES
Li1.05Fe0.95PO4
LiFePO4
J
I
H
*
G
F
E
D
C
B
A
Intensity (arb. units)
-20
-15
-10
-5
0
5
Energy Loss (eV)

Figure 4

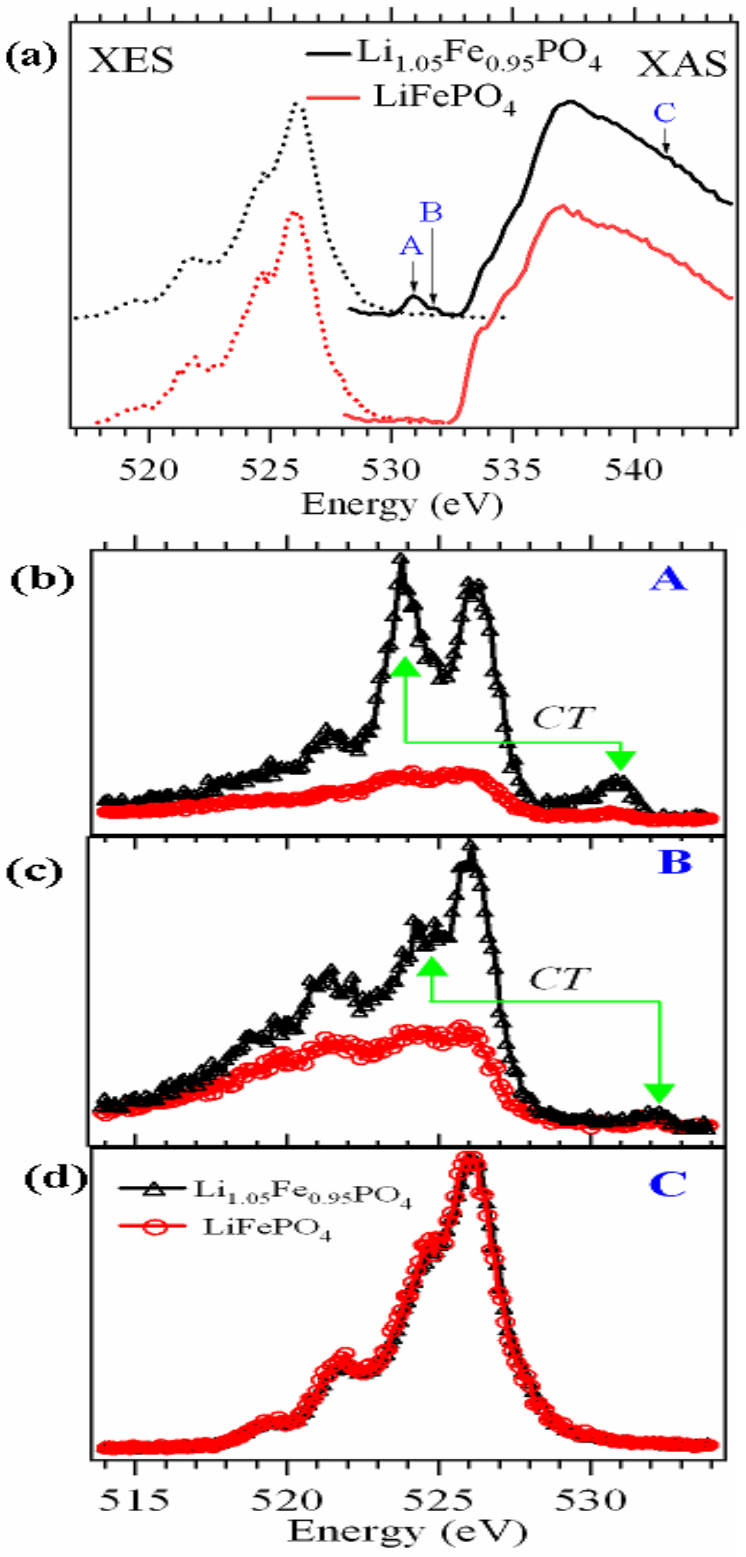
(a)
XES
Li1.05Fe0.95PO4
LiFePO4
XAS
A
B
C
520
525
530
535
540
Energy (eV)
(b)
A
CT
(c)
B
CT
(d)
Li1.05Fe0.95PO4
LiFePO4
C
515
520
525
530
Energy (eV)

Figure 5

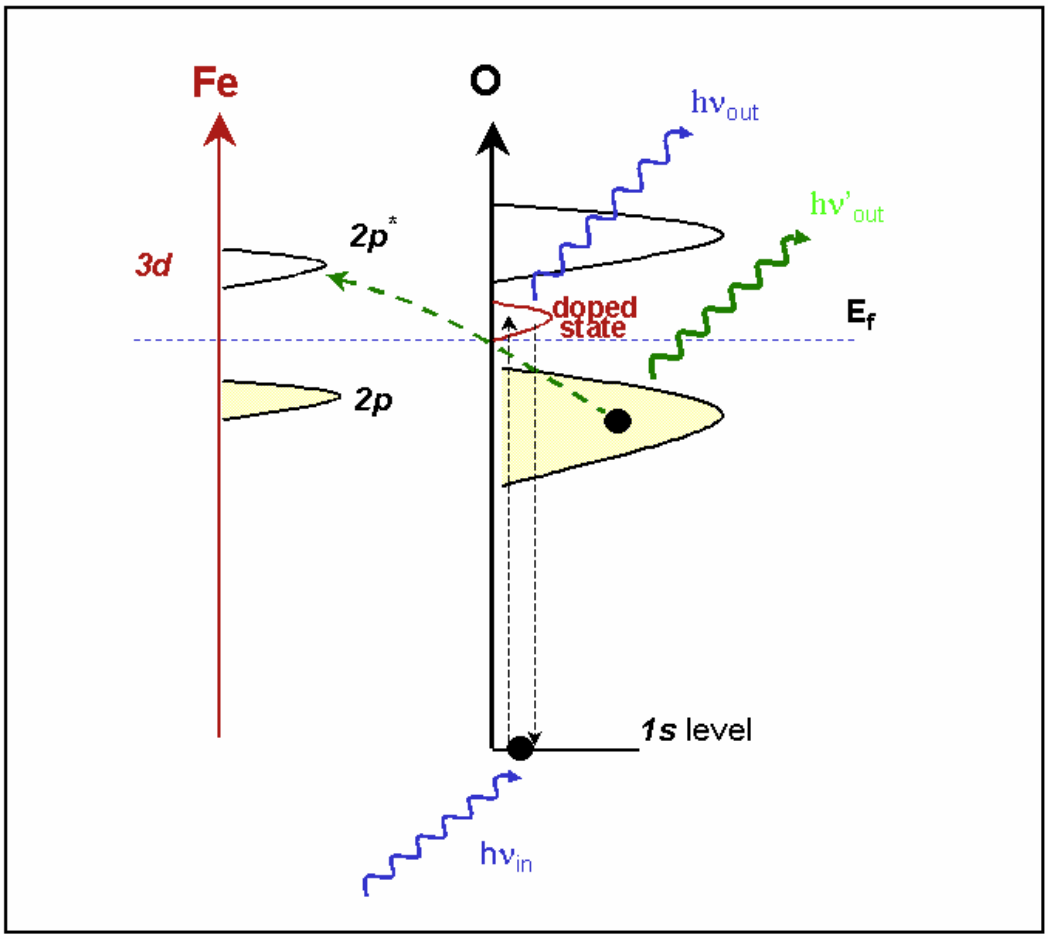

Figure 6